Pergamon

0094-114X(95)00056-9

Mech. Mach. Theory Vol. 31, No. 2, pp. 173–184, 1996

0094-114X/96 $15.00 + 0.00

A PHYSICAL MODEL OF THE SOLUTION SPACE AND THE ATLAS OF THE REACHABLE WORKSPACE FOR 2-DOF PARALLEL PLANAR MANIPULATORS

GAO FENG, ZHANG XIAO-QIU, ZHAO YONG-SHENG and WANG HONG-RUI

Robotic Research Center, Department of Mechanical Engineering, University of Yanshan, Qinhuangdao, Hebei 066004, People's Republic of China

(Received 24 May 1994; in revised form 3 April 1995; received for publication 26 June 1995)

Abstract—The paper presents a physical model of the solution space of 2-DOF parallel planar manipulators (PPM), investigates the theorem of the existing revolving input links, and systematically discusses the complete classification of the manipulators. It lays the foundation for future work to study the properties of the manipulators, because all of the significant properties can be represented as characteristic curves within the solution space. These will be presented in a forthcoming publication. The atlas of the reachable workspace areas for the 2-DOF PPMs is plotted.

1. INTRODUCTION

Conventional robot manipulators are generally of the serial type, i.e., their kinematic chains are simple and open. However, manipulators of this type present several drawbacks, the most important of which are: (a) only one of their motors is fixed, the remaining ones, accounting for a substantial part of the inertial load, are moving; (b) due to the cantilever-type of their links, their elastic flexibility is high, which introduces positioning inaccuracies and undesired dynamical side effects. As a means of overcoming the drawbacks of serial type industrial manipulators, parallel manipulators have been proposed. Potential benefits of parallel manipulators include higher stiffness and running speeds, plus lower power requirements and positioning errors, as well as allowing to fix all of their motor, or at least the heavier ones.

For this reason, closed-loop, inparallel-actuated robotic mechanisms have recieved a great deal of attention. Hunt [1, 2] and Tesar [3] provided a good introduction to various parallel robot structures. Gosselin [4], McCloy [5, 6], Bajpai [7], Asada [8] and Stoughtan [9] studied the workspace, mobility and methods for analysis and design of 2-DOF PPMs. And many researchers have investigated 3-DOF PPMs [10–12], spherical 3-DOF [11–13] and spatial 6-DOF [14–16] robotic manipulators.

Although many authors have considered parallel manipulators, none of them have paid attention to overall studying the relationships between the properties and the link-lengths of parallel robotic mechanisms. However, the relationships between the properties and the dimensions of planar 4-bar mechanisms were investigated [17–24].

This paper proposed the physical model of the solution space and the complete classification of 2-DOF PPMs, and lays the foundation for future work to study the properties of the manipulators. And the atlas of the reachable workspace areas for the 2-DOF PPMs is plotted.

2. PHYSICAL MODEL OF THE SOLUTION SPACE

2.1. Nondimensional parameters of 2-DOF PPMs

Figure 1 shows a typical 2-DOF PPMs. Where,

R_1 = length of the input bar

R_2 = length of the coupler bar

R_3 = length of the fixed bar (frame)

R_4 = length of the other coupler bar

R_5 = length of the other input bar

Because any of the link lengths of the manipulators lies in the range 0 to ∞, we must eliminate the physical size of the manipulators from the discussion. Let

$$L = (R_1 + R_2 + R_3 + R_4 + R_5)/4 \tag{1}$$

The lengths of bars $R_i (i = 1, 2, \ldots, 5)$ are divided by L to define five nondimensional parameters shown in Fig. 2 which are

$$r_i = R_i/L \quad (i = 1, 2, \ldots, 5) \tag{2}$$

Therefore, we can obtain

$$r_1 + r_2 + r_3 + r_4 + r_5 = 4 \tag{3}$$

The effect of normalizing the link lengths is to reduce a 5-dimensional space to a 4-dimensional one. In Gosselin's opinion [10], the parallel robotic manipulators should be symmetric, because the tasks to be performed by the manipulators are unknown and unpredictable a priori. Hence, by symmetry, the link lengths will be

$$R_5 = R_1, \quad R_4 = R_2 \tag{4}$$

Therefore,

$$r_5 = r_1, \quad r_4 = r_2 \tag{5}$$

This assumption will be used throughout. From equations (3) and (5), the relative lengths of the manipulators as shown in Fig. 2 have the following relationship:

$$2r_1 + 2r_2 + r_3 = 4 \tag{6}$$

The equations (5) and (6) can reduce a 5-dimensional space to a 2-dimensional one, which will be more convenient for what follows. Only finite positive values of the rs need to be considered.

2.2. Zero mobility planes

It is well known that a parallel 2-DOF maninpulator cannot be assembled if the length of the longest bar exceeds the sum of the lengths of the other four bars. If the length of the longest bar is equal to the sum of the lengths of the other four bars, the manipulator can be assembled, but the bars will not move. This is the zero mobility condition for the manipulators. Because any of the five bar lengths may be the longest, this leads to the three conditions as follows;

$$r_1 = 2, \quad r_2 = 2 \quad \text{and} \quad r_3 = 2 \tag{7}$$

which define three zero mobility planes.

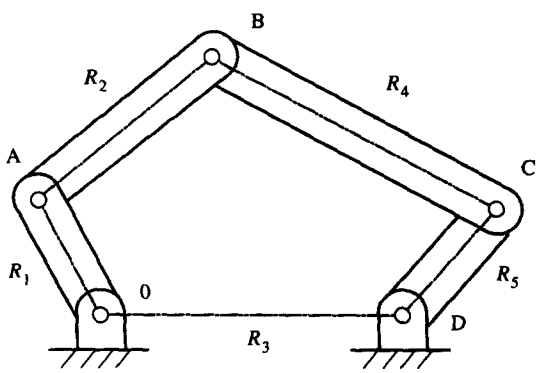

Fig. 1. Typical planar 2-DOF parallel robotic manipulator.

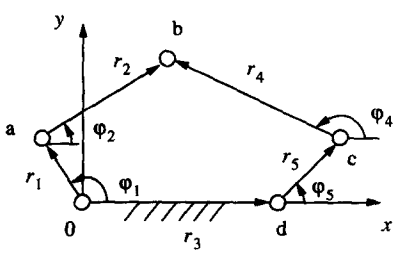

Fig. 2. The manipulator with nondimensional parameters.

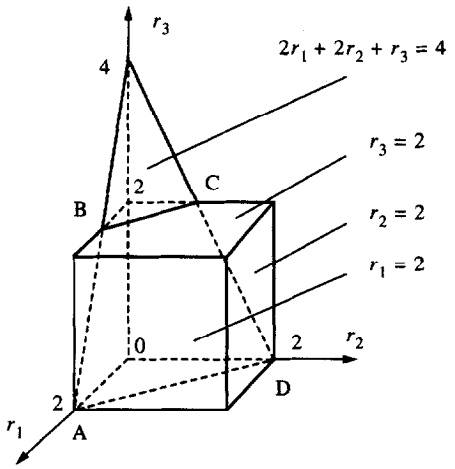

Fig. 3. Physical model of the solution space for the manipulators.

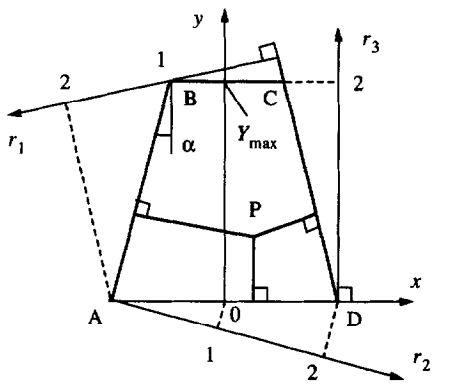

Fig. 4. Three-coordinate plane closed configuration.

2.3. Physical model of the solution space

Let r_1, r_2 and r_3 be the three orthogonal coordinate axes, respectively. Using equations (6), (7) and following conditions

$$r_1 > 0, \quad r_2 > 0, \quad r_3 \geqslant 0 \tag{8}$$

we can obtain the physical model of the solution space for the 2-DOF parallel manipulators as shown in Fig. 3, which is an isosceles trapezium ABCD. Any possible combination of the bar lengths is therefore represented by a particular set of r_1, r_2 and r_3 values on the trapezium ABCD.

3. PLANAR CLOSED CONFIGURATION WITH THREE COORDINATES $r_1r_2r_3$

For convenience, the physical model of the solution space that is the isosceles trapezium ABCD in the $r_1r_2r_3$ coordinate system as shown in Fig. 3 can be changed into the isosceles trapezium ABCD in the xy coordinate system as shown in Fig. 4, which is defined as the closed configuration of the solution space. We can use the following equations to calculate the values of x and y when the value of r_1, r_2 and r_3 are known, i.e.,

$$\begin{pmatrix} x \\ y \end{pmatrix} = \begin{pmatrix} Y_{max}/(2\cos\alpha) \\ 0 \end{pmatrix} - \begin{pmatrix} 1/\cos\alpha & 1/(4\cos\alpha) \\ 0 & -1 \end{pmatrix} \begin{pmatrix} r_1 \\ r_3 \end{pmatrix} \tag{9}$$

where

$$\alpha = \sin^{-1}(1/4)$$

$$Y_{max} = \text{the maximum value of } r_3.$$

In addition, if the values of x and y are known, the values of r_1, r_2 and r_3 can be calculated by

$$\begin{pmatrix} r_1 \\ r_2 \\ r_3 \end{pmatrix} = \begin{pmatrix} Y_{max}/2 \\ Y_{max}/2 \\ 0 \end{pmatrix} - \begin{pmatrix} \cos\alpha & 1/4 \\ -\cos\alpha & 1/4 \\ 0 & -1 \end{pmatrix} \begin{pmatrix} x \\ y \end{pmatrix} \tag{10}$$

4. THE THEOREM FOR DETERMINING THE EXISTING REVOLVING LINKS

4.1. The kinematic influence coefficients for angular velocities

In order to derive the kinematic influence coefficients of the 2-DOF parallel manipulator, we consider the manipulator shown in Fig. 2. Writing its loop closure equation, one obtains

$$r_1 e^{i\varphi_1} + r_2 e^{i\varphi_2} - r_3 - r_4 e^{i\varphi_4} - r_5 e^{i\varphi_5} = 0 \tag{11}$$

Since

$$\begin{pmatrix}\dot{\varphi}_2\\ \dot{\varphi}_4\end{pmatrix}=[G]\begin{pmatrix}\dot{\varphi}_1\\ \dot{\varphi}_5\end{pmatrix}$$

where, $[G]$ is the matrix of the kinematic influence coefficients, i.e.

$$[G]=\begin{bmatrix}\dfrac{\partial\varphi_2}{\partial\varphi_1} & \dfrac{\partial\varphi_2}{\partial\varphi_5}\\ \dfrac{\partial\varphi_4}{\partial\varphi_1} & \dfrac{\partial\varphi_4}{\partial\varphi_5}\end{bmatrix} \tag{12}$$

The angular velocities of input links r_1 and r_5 are obtained as

$$\begin{pmatrix}\dot{\varphi}_1\\ \dot{\varphi}_5\end{pmatrix}=[G]^{-1}\begin{pmatrix}\dot{\varphi}_2\\ \dot{\varphi}_4\end{pmatrix} \tag{13}$$

Partially differentiating equation (11) with respect to φ_1 and φ_5 respectively, leads to

$$[G]^{-1}=\begin{pmatrix}r_2r_5\sin(\varphi_5-\varphi_2) & r_4r_5\sin(\varphi_4-\varphi_5)\\ r_1r_2\sin(\varphi_1-\varphi_2) & r_1r_4\sin(\varphi_4-\varphi_1)\end{pmatrix}\frac{1}{r_1r_5\sin(\varphi_1-\varphi_5)} \tag{14}$$

The elements of the matrix $[G]^{-1}$ are only functions of the position parameters of the manipulators.

4.2. The extreme positions of links r_1 and r_5

When the input links r_1 and r_5 are located at the extreme positions and the angular velocities $\dot{\varphi}_2$ and $\dot{\varphi}_4$ are not equal to zero, the angular velocities of links r_1 and r_5 must be equal to zero, that is

$$\dot{\varphi}_1=0,\quad \dot{\varphi}_5=0 \tag{15}$$

Therefore, the elements of matrix $[G]^{-1}$ have to be equal to zero, and we can obtain the following conditions:

$$\dot{\varphi}_1=0,\quad \varphi_5-\varphi_2=0 \text{ or } \pm\pi, \quad \text{and} \quad \varphi_4-\varphi_5=0 \text{ or } \pm\pi \tag{16}$$

$$\dot{\varphi}_5=0,\quad \varphi_1-\varphi_2=0 \text{ or } \pm\pi, \quad \text{and} \quad \varphi_4-\varphi_1=0 \text{ or } \pm\pi \tag{17}$$

Using equations (16) and (17), we can determine the extreme positions of links r_1 and r_5, respectively. From equations (16), if

$$\varphi_4=\varphi_5,\quad \varphi_2=\pi+\varphi_5 \tag{18}$$

substituting equations (18) into (11), we can obtain

$$r_1e^{i\varphi_1}-r_3=(r_2+r_4+r_5)e^{i\varphi_5} \tag{19}$$

Solving equation (19), one of the extreme positions of link r_1 is given by, as shown in Fig. 5(a),

$$\cos\varphi_1=[r_1^2+r_3^2-(r_2+r_4+r_5)^2]/(2r_1r_3) \tag{20}$$

If

$$\varphi_2=\varphi_5,\quad \varphi_4=\pi+\varphi_5 \tag{21}$$

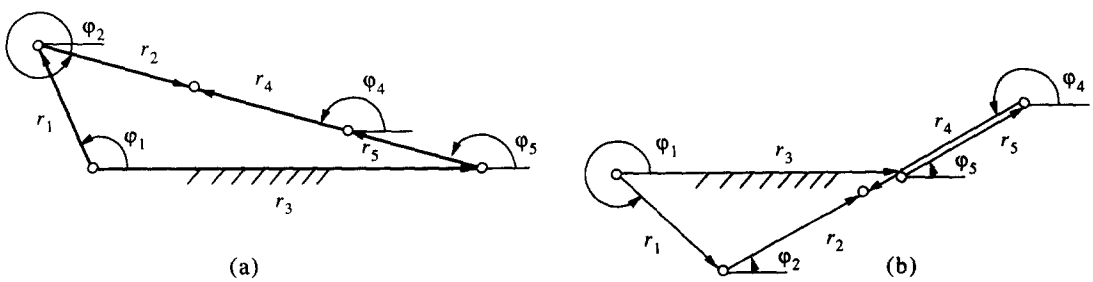

Fig. 5. Two extreme positions of link r_1. (a) $\varphi_4=\varphi_5$, $\varphi_2=\pi+\varphi_5$, (b)$\varphi_2=\varphi_5$, $\varphi_4=\pi+\varphi_5$

then

$$r_1 e^{i\varphi_1} - r_3 = (r_5 - r_4 - r_2)e^{i\varphi_5} \tag{22}$$

Solving equation (22), the other extreme position of link r_1 is obtained by, as shown in Fig. 5(b),

$$\cos\varphi_1 = [r_1^2 + r_3^2 - (r_5 - r_4 - r_2)^2]/(2r_1 r_3) \tag{23}$$

Using equation (17), we can also derive the equation for calculating the extreme positions of link r_5, i.e., if $\varphi_2 = \varphi_1$ and $\varphi_4 = \pi + \varphi_1$, then

$$\cos(\pi - \varphi_5) = [r_5^2 + r_3^2 - (r_1 + r_2 + r_4)^2]/(2r_1 r_3) \tag{24}$$

If $\varphi_4 = \varphi_1$, $\varphi_2 = \pi - \varphi_1$, then

$$\cos(\pi - \varphi_5) = [r_5^2 + r_3^2 - (r_1 - r_2 - r_4)^2]/(2r_5 r_3) \tag{25}$$

4.3. The theorems for determining existing revolving input links r_1 and r_5

If the manipulator shown in Fig. 2 satisfies equations (20), (23), (24) and (25), the revolving input links do not exist. On the contrary, if it does not satisfy equation (20), (23)–(25), the theorems for determining the existing revolving input links can be obtained as follows:

$$|[r_1^2 + r_3^2 - (r_1 + 2r_2)^2]/(2r_1 r_3)| > 1 \tag{26}$$

and

$$|[r_1^2 + r_3^2 - (r_1 - 2r_2)^2]/(2r_1 r_3)| > 1 \tag{27}$$

If the manipulator shown in Fig. 2 satisfies the conditions (26) and (27) at the same time, links r_1 and r_5 all can rotate through a full revolution.

5. COMPLETE CLASSIFICATION

5.1. Change point parallel 2-DOF manipulation (CPM)

If a parallel manipulator shown in Fig. 2 satisfies one of the following conditions,

$$|[r_1^2 + r_3^2 - (r_1 + 2r_2)^2]/(2r_1 r_3)| = 1 \tag{28}$$

and

$$|[r_1^2 + r_3^2 - (r_1 - 2r_2)^2]/(2r_1 r_3)| = 1 \tag{29}$$

the manipulator is designated as the CPM. Physically this means that all five bars can be colinear and therefore, may require special attention to pass through a change point position. From equations (28) and (29), we can derive three conditions for determining the CPMs, i.e.:

If $r_1^2 + r_3^2 < (r_1 + 2r_2)^2$, using equation (28), we obtain $(r_1 + 2r_2)^2 = (r_1 + r_3)^2$, so

$$2r_2 = r_3 \tag{30}$$

If $r_1^2 + r_3^2 < (r_1 - 2r_2)^2$, from equation (29), we can derive

$$(r_1 - 2r_2)^2 = (r_1 + r_3)^2 \tag{31}$$

When $r_1 < 2r_2$, using equation (4), equation (31) can be rewritten in the form

$$2r_2 = 2r_1 + r_3 \quad \text{or} \quad r_2 = 1 \tag{32}$$

If $r_1^2 + r_3^2 > (r_1 - 2r_2)^2$, using equation (29), one has

$$(r_1 - r_3)^2 = (r_1 - 2r_2)^2 \tag{33}$$

If $r_1 > r_3$ and $r_1 > 2r_2$, or $r_1 < r_3$ and $r_1 < 2r_2$, from equation (33), we obtain $r_3 = 2r_2$, which is the same as equation (30). If $r_1 > r_3$ and $r_1 < 2r_2$, or $r_1 < r_3$ and $r_1 > 2r_2$, by means of equation (30), we can yield

$$2r_1 = 2r_2 + r_3, \quad \text{or} \quad r_1 = 1 \tag{34}$$

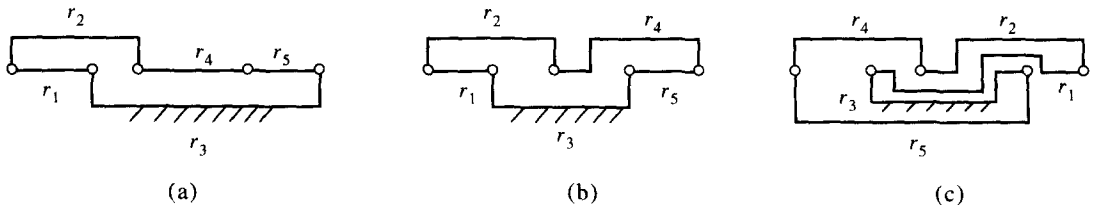

Fig. 6. Three types of CPMs. (a) $2r_2 = r_3$, (b)$r_2 = 1$, (c) $r_1 = 1$.

The manipulators which satisfy conditions (30), (32) and (34) are shown in Fig. 6, respectively.

From equations (30), (32) and (34), lines 1, 2 and 3 can be drawn on the closed configuration as shown in Fig. 7. These three lines are called change point lines, which divide the closed configuration ABCD into five parts I, II_1, II_2, III_1 and III_2

5.2. Unrestrained double crank parallel manipulators (UDCM)

According to conditions (26) and (27), we can define the region of the UDCMs on the solution space. This kind of manipulators (UDCMs) have two input links r_1 and r_5 which can rotate through a full revolution freely.

Using equation (26), if $r_1^2 + r_3^2 > (r_1 + 2r_2)^2$, one can obtain $(r_1 + 2r_2)^2 > (r_1 + r_3)^2$, that is

$$2r_2 > r_3 \tag{35}$$

If $r_1^2 + r_3^2 > (r_1 + 2r_2)^2$, we cannot find any manipulators which satisfy equation (26). The manipulators on the regions I, II_1 and II_2 as shown in Fig. 7 are content with equation (35).

In addition, if $(r_1 - 2r_2)^2 > r_1^2 + r_3^2$, by means of condition (27), we can obtain

$$(r_1 - 2r_2)^2 > (r_1 + r_3)^2 \tag{36}$$

when $r_1 < 2r_2$, equation (36) can be rewritten as

$$2r_2 > 2r_1 + r_3 \quad \text{or} \quad r_2 > 1 \tag{37}$$

Therefore, from Fig. 7 and equations (35) as well as (37), we can see that all of the UDCMs must be located in region I.

5.3. Restrained double crank 2-DOF parallel manipulators (RDCM)

If a 2-DOF parallel manipulator does not satisfy equation (36) but (35), it is called RDCM. There are two types of manipulators which are located in regions II_1 and II_2 as shown in Fig. 7 and have double cranks under given conditions.

When $\varphi_5 = \pi$ or $\varphi_1 = 0$, the remaining part of the 2-DOF manipulator can be considered as the 4-bar mechanism. By means of Grashof's theorem, we can prove that the manipulators in region II_1 satisfy the following statement:

If $\varphi_5 = \pi$ or $\varphi_1 = 0$, input link r_1 or r_5 can rotate though a full revolution; and if $\varphi_5 = 0$ or $\varphi_1 = \pi$, input link r_1 or r_5 can not rotate though a full revolution.

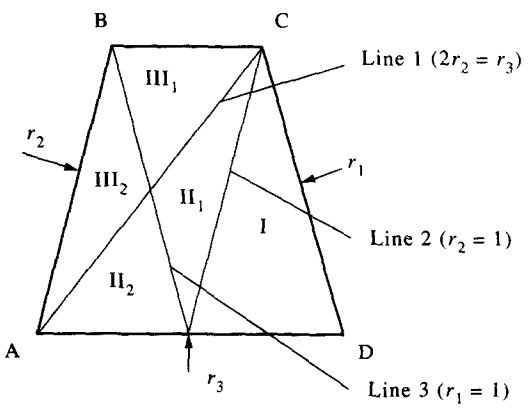

Fig. 7. Three lines of change point manipulators.

Table 1. Complete classification of 2-DOF PPMs

Number	Region	Symbol	Dimensional properties
1	I	UDCM	$r_2 > 1$
2	II_1	RDCM	$r_2 < 1,\ r_1 < 1,\ 2r_2 > r_3$
	II_2	RDCM	$2r_2 > r_3,\ r_1 > 1$
3	III_1	DRM	$2r_2 < r_3,\ r_1 < 1$
	III_2	DRM	$2r_2 < r_3,\ r_1 > 1$
4	line 1	CPM	$2r_2 = r_3$
	line 2	CPM	$r_2 = 1$ or $2r_2 = r_3 + 2r_1$
	line 3	CPM	$r_1 = 1$ or $2r_1 = r_3 + 2r_2$

However, the manipulators in region II_2 do not satisfy the above statement, but under some specific conditions, such as $\varphi_1 = \varphi_5$ in the whole motion cycle, the manipulators can have two cranks r_1 and r_5, too.

5.4. Double rocker 2-DOF parallel manipulators (DRM)

If input links r_1 and r_5 of the manipulator cannot rotate through a full revolution in any case, the manipulator is called DRM. From equations (20) and (24), one can obtain the condition of determining DRMs as follows:

$$|[r_1^2 + r_3^2 - (r_1 + 2r_2)^2]/(2r_1 r_3)| < 1 \tag{38}$$

when $(r_1 + 2r_2)^2 > r_1^2 + r_3^2$, equation (38) can be rewritten as $(r_1 + 2r_2)^2 < (r_1 + r_3)^2$. Therefore,

$$2r_2 < r_3 \tag{39}$$

As shown in Fig. 7, all of DRMs are located in regions III_1 and III_2.

Table 1 shows the complete classification of the 2-DOF parallel manipulators, which have four types: UDCM, RDCM, DRM and CPM.

6. EXPRESSIONS FOR CALCULATION OF REACHABLE WORKSPACE AREAS OF RELATIVE 2-DOF PPMs

Using equations (1) and (2), one can change a real 2-DOF PPM with dimensional parameters $R_i (i = 1, 2, \ldots, 5)$ into a relative 2-DOF PPM with nondimensional $r_i (i = 1, 2, \ldots, 5)$. Therefore, its reachable workspace considered here is also nondimensional and the workspace-area values of relative 2-DOF PPMs are related to R, r and r_3, where

$$R = r_1 + r_2, \quad r = |r_1 - r_2| \tag{40}$$

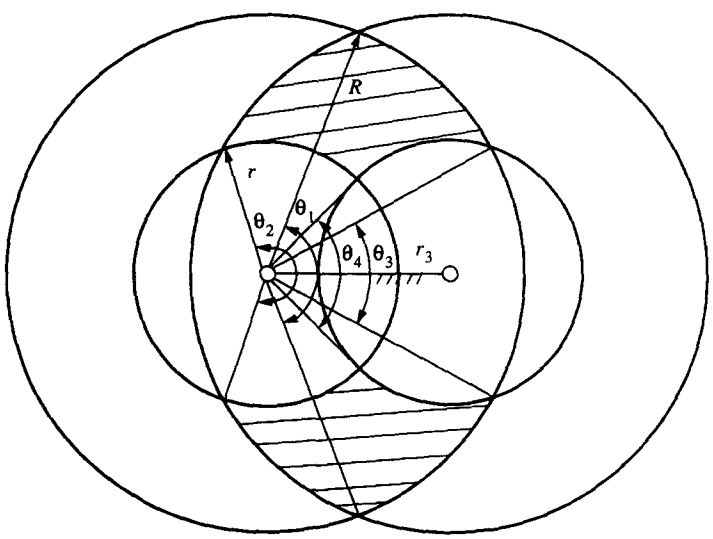

Fig. 8. The workspace shape of case 1.

Table 2. Dimensional properties of the five cases of the workspace areas

Number	Case i	Symbol	Dimensional properties
1	1	C_{1a}	$r_3 > 2r_2,\ r_1 > r_2,\ r_1 > 1$
2	1	C_{1b}	$r_3 > 2r_1,\ r_1 < r_2,\ r_2 > 1$
3	2	C_{2a}	$r_3 > 2r_2,\ r_3 < 2r_1,\ r_1 < 1$
4	2	C_{2b}	$r_3 > 2r_1,\ r_3 < 2r_2,\ r_2 < 1$
5	3	C_{3a}	$r_3 < 2r_2,\ r_1 > r_2,\ r_1 > 1$
6	3	C_{3b}	$r_3 < 2r,\ r_1 < r_2,\ r_2 > 1$
7	4	C_{4a}	$r_3 < 2r_2,\ r_1 > r_2,\ r_1 < 1$
8	4	C_{4b}	$r_3 < 2r_1,\ r_1 < r_2,\ r_2 < 1$
9	5	C_{5a}	$r_3 > 2r_1,\ r_1 > r_2$
10	5	C_{5b}	$r_3 > 2r_2,\ r_1 < r_2$

The expressions for calculation of the workspace areas have five cases as follows.

CASE 1: $r_3 < 2r$ and $(r_3 + r) > R > (r_3 - r)$
When a 2-DOF PPM satisfies the conditions

$$r_3 < 2r \quad \text{and} \quad (r_3 + r) > R > (r_3 - r) \tag{41}$$

its reachable workspace is the shadow area which is two unconnected zones as shown in Fig. 8. From Fig. 8, the workspace area can be calculated by

$$A_{\text{case 1}} = A_1 - A_2 - A_3 + A_4 \tag{42}$$

where

$$\begin{aligned} A_1 &= R^2\theta_1 - b_1\sqrt{R^2 - (b_1/2)^2} \\ A_2 &= r^2\theta_2 - b_2\sqrt{r^2 - (b_2/2)^2} \\ A_3 &= R^2\theta_3 - b_3\sqrt{R^2 - (b_3/2)^2} \\ A_4 &= r^2\theta_4 - b_4\sqrt{r^2 - (b_4/2)^2} \end{aligned} \tag{43}$$

here,

$$\begin{aligned} \theta_1 &= 2\cos^{-1}[r_3/(2R)] \\ \theta_2 &= 2\cos^{-1}[(r^2 + r_3^2 - R^2)/(2rr_3)] \\ \theta_3 &= 2\cos^{-1}[(R^2 + r_3^2 - r^2)/(2Rr_3)] \\ \theta_4 &= 2\cos^{-1}[r_3/(2r)] \end{aligned} \tag{44}$$

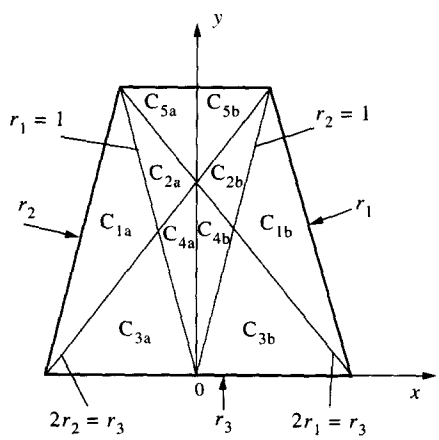

Fig. 9. Distribution of the five cases on the physical model.

and

$$b_1 = 2R \sin(\theta_1/2)$$
$$b_2 = 2r \sin(\theta_2/2)$$
$$b_3 = 2R \sin(\theta_3/2)$$
$$b_4 = 2r \sin(\theta_4/2) \tag{45}$$

Substituting equations (45) into (43), equations (43) can be rewritten as

$$A_1 = R^2(\theta_1 - \sin\theta_1)$$
$$A_2 = r^2(\theta_2 - \sin\theta_2)$$
$$A_3 = R^2(\theta_3 - \sin\theta_3)$$
$$A_4 = r^2(\theta_4 - \sin\theta_4) \tag{46}$$

CASE 2: $r_3 > 2r$ and $(r_3 + r) > R > (r_3 - r)$
If the 2-DOF PPMs are contented with the conditions

$$r_3 > 2r \quad \text{and} \quad (r_3 + r) > R > (r_3 - r) \tag{47}$$

the angle θ_4 is equal to zero, i.e.

$$\theta_4 = 0 \quad \text{and} \quad A_4 = 0 \tag{48}$$

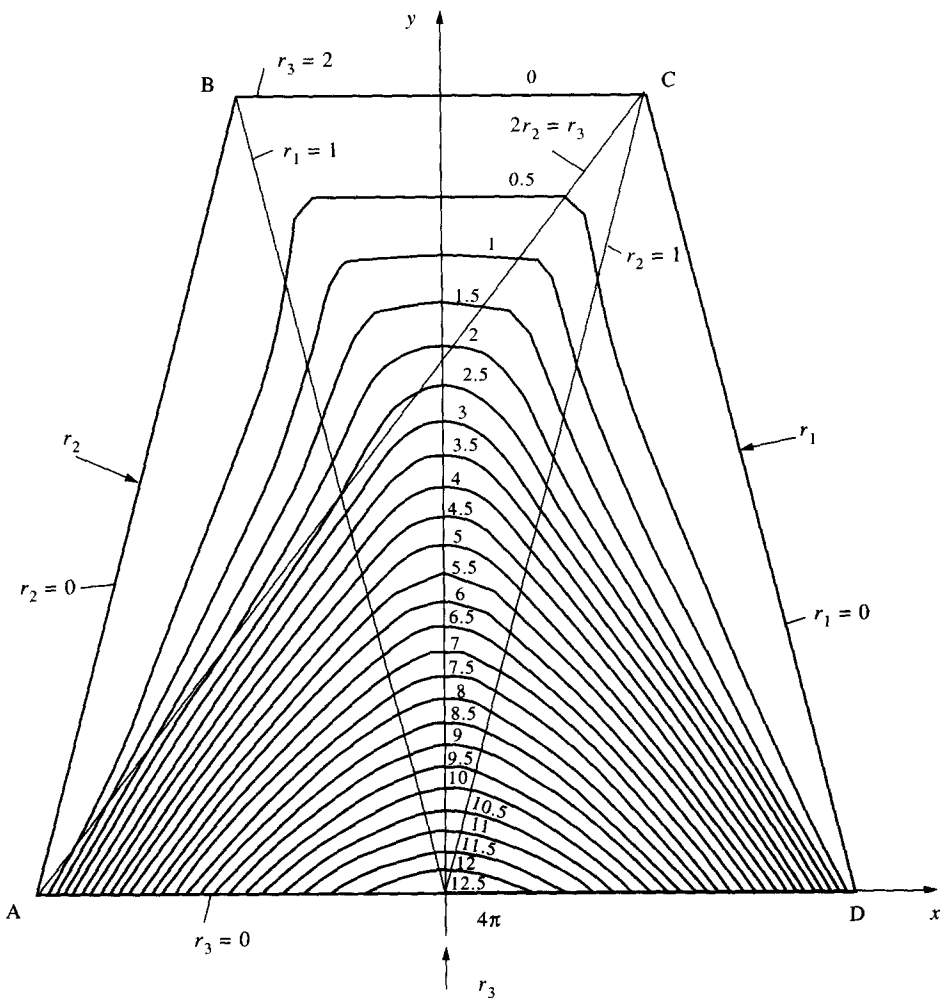

Fig. 10. The workspace-area-property atlas of 2-DOF PPMs.

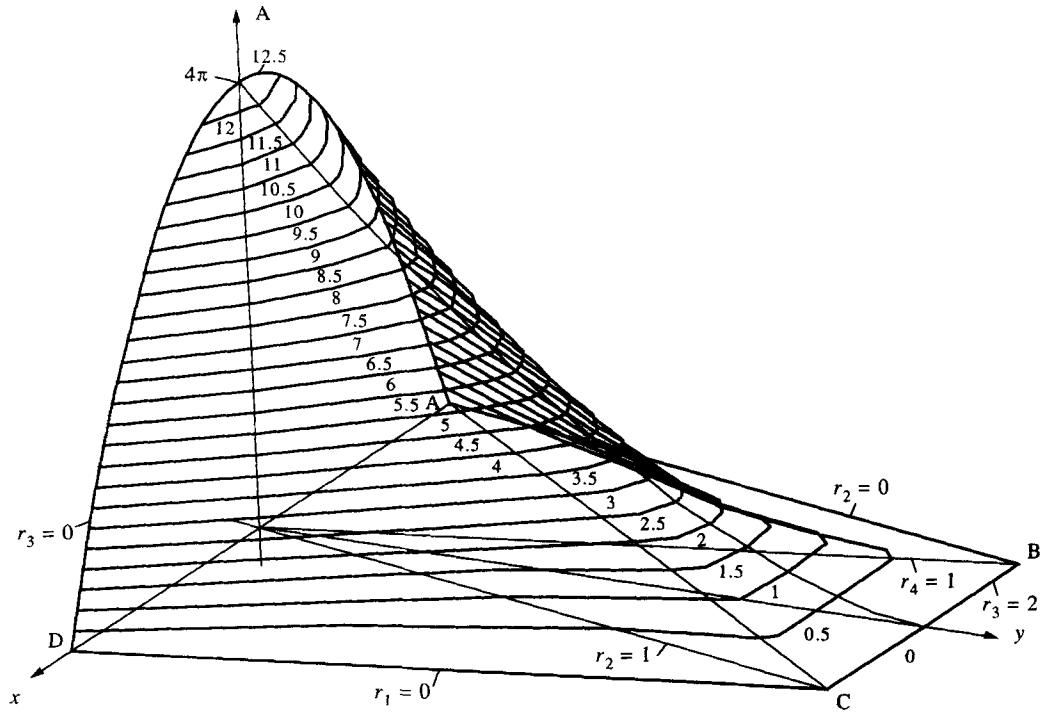

Fig. 11. The 2-D figure of the workspace-area property.

Therefore, the workspace areas of the 2-DOF PPMs can be computed by equation (42), that is

$$A_{\text{case 2}} = A_1 - A_2 - A_3$$
$$= R^2(\theta_1 - \sin\theta_1 - \theta_3 + \sin\theta_3) - r^2(\theta_2 - \sin\theta_2) \tag{49}$$

CASE 3: $r_3 < 2r$ and $R > (r_3 + r)$
If the 2-DOF PPMs satisfy the conditions

$$r_3 < 2r \quad \text{and} \quad R > (r_3 + r) \tag{50}$$

we can see

$$\theta_2 = 2\pi \quad \text{and} \quad \theta_3 = 0 \tag{51}$$

Therefore, by means of equations (7) and (16), the workspace areas of this kind of a 2-DOF PPMs can be computed as

$$A_{\text{case3}} = A_1 - A_2 + A_4$$
$$= R^2(\theta_1 - \sin\theta_1) - 2\pi r^2 + r^2(\theta_4 - \sin\theta_4) \tag{52}$$

CASE 4: $r_3 > 2r$ and $R > (r_3 + r)$
If a kind of 2-DOF PPMs satisfy the following conditions

$$r_3 > 2r \text{ and } R > (r_3 + r) \tag{53}$$

we can see that

$$\theta_2 = 2\pi, \quad \theta_3 = 0 \quad \text{and} \quad \theta_4 = 0 \tag{54}$$

Therefore, the workspace areas of this kind of 2-DOF PPMs can be determined by

$$A_{\text{case4}} = A_1 - A_2$$
$$= R^2(\theta_1 - \sin\theta_1) - 2\pi r^2 \tag{55}$$

CASE 5: $r_3 > 2r$ and $R < (r_3 - r)$
If the 2-DOF PPMs satisfy the following conditions

$$r_3 > 2r \quad \text{and} \quad R < (r_3 - r) \tag{56}$$

we can see that

$$\theta_2 = 0, \quad \theta_3 = 0 \quad \text{and} \quad \theta_4 = 0 \tag{57}$$

Therefore, the workspace areas of this kind of 2-DOF PPMs can be calculated by

$$A_{\text{case } 5} = A_1 = R^2(\theta_1 - \sin\theta_1) \tag{58}$$

7. RELATIONSHIP BETWEEN THE REAL AND THE RELATIVE WORKSPACE AREAS

When a real 2-DOF PPM has the links $R_i (i = 1, 2, , \ldots, 5)$, by equations (1) and (42), the workspace area A_{real} of the real 2-DOF PPM can be calculated by

$$A_{\text{real}} = A_{\text{case } i} L^2 \tag{59}$$

where $A_{\text{case } i}$ is the workspace area of the relative 2-DOF PPM with links $r_i (i = 1, 2, \ldots, 5)$; and L can be calculated by equation (1).

Equation (59) expresses the relationship between the real and the relative workspace areas of 2-DOF PPMs.

8. DISTRIBUTION OF THE ABOVE FIVE CASES IN THE PHYSICAL MODEL OF THE SOLUTION SPACE

The dimensional property of these five cases is shown in Table 2. The five types of 2-DOF PPMs in five cases occupy the different regions within the physical model of the solution space as shown in Fig. 9, respectively. By means of Table 2 and Fig. 9, we can obviously see the relationship between the workspace shapes and the link lengths of the relative 2-DOF PPMs which are symmetrical about axis y in an orderly fashion.

9. THE VALUES OF THE WORKSPACE AREAS AND THEIR DISTRIBUTION WITHIN THE PHYSICAL MODEL

By equations (42), (49), (52), (55) and (58), all values of the workspace areas of 2-DOF PPMs can be calculated and the locus with the same values of the workspace areas can be plotted within the physical model of the solution space, as shown in Fig. 10, so the workspace-area-property atlas is obtained. At the same time, we also plot the 3-D figure of the workspace area as shown in Fig. 11, where plane xy expresses the surface of the physical model, and axis A represents the values of the workspace areas.

From Figs 10 and 11, one can clearly see the following regularities:

- The values of the workspace areas are symmetrical about axis y.
- The values of the workspace areas reduce along with $r_3(y)$ increasing.
- If $r_3 = 0$ $(y = 0)$ and $r_1 = r_2 = 0$ $(x = 0)$, the workspace area has the maximum value, that is, $A_{\max} = 4\pi$.

10. CONCLUSION

This paper establishes the physical model of the solution space for the parallel 2-DOF planar robotic manipulators, which is one isosceles trapezium, investigates the theorem of the existing revolving input links, and systematically discusses the classification, which has four types: UDCM, RDCM, DRM, and CPM. It lays the foundation for future work to study the properties of the parallel manipulators, because all of the significant properties can be represented as characteristic curves within the solution space.

And we use the physical model of the solution space to investigate the relationship between the values of the workspace areas and the relative link lengths of 2-DOF PPMs. By the aid of a computer, the values of the workspace areas of all the manipulators are calculated and plotted on the physical model, so the workspace-area-property atlas is obtained. The atlas is very useful for designers overall to understand and know well the relationship between the workspace property and the dimensions of all the 2-DOF parallel planar manipulators.

REFERENCES

1. K. H. Hunt, *J. Mech. Transmissions Automatn Design* **105,** 705–712 (1983).
2. K. H. Hunt, *Mech. Engng Trans. Inst. Engnrs* **MET,** 213–220 (1982).
3. D. Tessar and M. S. Butler, *Manufacturing Rev.* **2,** 91–118 (1989).
4. C. M. Gosselin and M. Guillot, *Trans. ASME J. Mech Design* **113,** 451–455 (1991).
5. D. NcCloy, *Robotica* **8,** 355–362 (1990).
6. D. McCloy, *The 4th Conf. of the Irish Manufacturing Committee*, Limerick, Ireland (1987).
7. A. Bajpai and B. Roth. *Int. J. Robotics Res.* 131–142 (1986).
8. H. Asada and K. Youcef-Toumi, *American Control Conf.*, San Diego (1984).
9. R. Stoughton and T. Kokkinis, *ASME Design Automation Conf.* **DET-Vol. 10-2,** 73–79 (1987).
10. C. Gosselin and J. Angeles, *J. Mech. Transmission Automatn Design* **110,** 35–41 (1988).
11. C. Gosselin and J. Angeles, *Trans. ASME J. Mech. Design* **112,** 494–500 (1990).
12. M. Thomas, H. C. Yuan-Chou and D. Tesar, *J. Mech. Transmission Automatn Design* **107,** 163–169 (1985).
13. C. Gosselin and J. Angeles, *Trans. ASME J. Mech. Transmissions Automatn Design* **111,** 202–207 (1989).
14. Z. Huang and Y. Y. Qu, *Proc. of the 8th World Congress on TMM (IFToMM)* 991–994 (1991).
15. Z. Huang and H. B. Wang, ASME. Paper 86-DET-168 (1986).
16. C. Gosselin, *Trans. ASME J. Mech. Design* **112,** 331–336 (1990).
17. Yang Ji-Hou, *Mech. Mach. Theory* **22,** 71–76 (1987).
18. Wang Cheng-Yun and Yang Ji-Hou, *Chin. J. Mech. Engng* **27** (1991).
19. C. R. Barker, *Mech. Mach. Theory* 535–554 (1985).
20. C. R. Barker, ASME. Paper 84-DET-126, and 84-DET-127 (1984).
21. C. R. Barker and Y. R. Teng. *Mech. Mach. Theory* **20,** 329–344 (1985).
22. T. H. Davies, J. E. Bake, and A. G. R. Thompson, *Mech. Mach. Theory* **14,** 389–403 (1979).
23. C. R. Barkar. *Mech. Mach. Theory* **22,** 351–358 (1987).
24. Yang Ji-Hou and Gao Feng *The 4th IFToMM. Int. Sym. on Linkages and CAD Methods*, Vol. I-1, Paper. 19, pp. 14–152 (1985).

ФИЭИЧЕСКИЙ МОДЕЛВ И ВСЕ ВИДПО ПРОСТРАНСТВЕ РЕШЕНИЯ ПЛОСКИХ РОБОТОВ ПАРАЛЛЕЛВНОГО СОЕДИНЕНИЯ С ДВУМЯ СВОБ ОДЫ

Реферат—Настоящой статы основана фиэигеская моделв плоских роботов папаллельного соединения с двумя степе ней свободы и рассмотрены услоия существовсищя кривоцина для входящего эвена, систематически обсуждёны все виды механиэма робота, потому что на модели пространства решения можно рисовать раэны лихии свойства и характерной о собенности, которые имеют эначимость.

В будущей статье будет рассмотреть по этим работам.